Comminution process modeling based on the monovariate and bivariate direct quadrature method of moments

Christine Frances, Alain Liné

Comminution Process Modeling Based on the Monovariate and Bivariate Direct Quadrature Method of Moments

Christine Frances
Université de Toulouse, INPT, UPS, LGC (Laboratoire de Génie Chimique), 4 Allée Emile Monso, BP 84234, 31432 Toulouse Cedex 4, France

CNRS, LGC (Laboratoire de Génie Chimique), F-31432 Toulouse Cedex 4, France

Alain Liné
Université de Toulouse, INSA, LISBP (Laboratoire d'Ingénierie des Systèmes Biologiques et Procédés), 135 Avenue de Rangueil, 31077 Toulouse Cedex 4, France

CNRS, LISBP (Laboratoire d'Ingénierie des Systèmes Biologiques et Procédés), F-31077 Toulouse Cedex, France

INRA, LISBP (Laboratoire d'Ingénierie des Systèmes Biologiques et Procédés), F-31077 Toulouse Cedex, France

DOI 10.1002/aic.14358

Population balance equations (PBE) applied to comminution processes are commonly based on selection and breakage functions, which allow the description of changes of particle-size distributions vs. time. However, other properties, such as the particle strength, also influence the grinding kinetics. A bivariate PBE was developed and resolved by the direct quadrature method of moments. This equation includes both the particle size and strength, the latter of which is defined as the minimum energy required for breakage. The monovariate case was first validated by comparing the predicted moments with those calculated from the size distributions given by an analytical solution of the PBE derived for specific selection and breakage functions. The bivariate model was then compared with a discretized model to evaluate its validity. Finally, the benefit of the bivariate model was proven by analyzing the sensitivity of some parameters and compar-ing the results of the monovariate and bivariate cases.

Keywords: particle technology, mathematical modeling, grinding, population balance, direct quadrature method of moments

Introduction

Population balance equations (PBE) are commonly used to model particulate processes. In the framework of comminution processes, PBE tracks the change in the density distribution of the weight of particles distributed over defined size classes. Batch grinding mass balance equations usually incorporate the selection function, which expresses the breakage probability of particles as a function of their size, and the breakage function, which describes the daughter particle-size distribution. This approach permits the optimization of the size reduction process and has intensively been used in the past to model ball mills[1,2] and more recently to help determine breakage and selection functions parameters.[3,4] The kinetics parameters are then back-calculated from the PBE. A similar approach was also used to model the simultaneous breakage and reagglomeration of fines in a grinding process[5] and to identify the grinding mechanisms in a submicron milling process.[4,6] The modeling of continuous grinding processes is also based on PBE, which combines the fragmentation kinetics with the particle residence time distribution. The batch mass balance equation is first solved, which yields the temporal change of the mass fractions in each size class. The grinding kinetics is then combined with a global transport model to obtain the size distribution of the ground product during a continuous process.[7] Many analytical or approximated solutions of the batch grinding equation have been proposed in the literature[2,8] depending on the specific forms of the selection and breakage functions. Irrespective of the method used to solve the mass balance equation, the mass balance can describe the fragment-size distribution as a function of the grinding time.

However, size is not the only important solid characteristic in a grinding process, as the particle strength (or grindability) is another key parameter that directly affects the process kinetics. Grindability can be the cause of what Austin et al.[9] called an abnormal breakage behavior, which is characterized by an increase in the selection function vs. time (when a fatigue phenomenon occurs) or a decreasing tendency (when small fragments are more resistant than larger ones).

Correspondence concerning this article should be addressed to C. Frances at Christine.Frances@ensiacet.fr.

The usefulness of the actual population balance models for mill design, optimization, or control is thus reduced if the particle size is the unique property. An innovative approach was recently proposed by Crespo,[10] who developed a PBE for a ball-milling process in which the weight distribution was jointly characterized by the particle size and strength. In the context of grinding processes, the particle strength can be practically defined by expressing the minimum energy required to break the particle. Such a property can be evaluated by performing crushing tests on a single particle, such as with the ultrafast load cell (UFCL).[11,12] The method used to characterize the fracture energy leads to a statistical treatment of the results to consider the variability of the particle properties. The particle strength is thus defined by an energy spectrum that depends on particle size. The PBE applied to comminution processes can finally be written for the breakage energy-size distribution.

An important quantity for grinding processes is the energy consumed by the mill, a part of which is transmitted to the particles. For example, Kwade[13] developed theoretical considerations of interactions between the fracture energy spectra induced by bead motion to characterize the material properties and impact energy for stirred media mills. The impact energy spectra depend on the process conditions and can be determined by computing the collision energy via the discrete element method,[14,15] simulating the hydrodynamics inside the grinding chamber using computation fluid dynamics (CFD) codes based on Reynolds-averaged Navier–Stokes[16] or direct numerical simulation.[17] Thus, a first main challenge of comminution processes modeling is to simultaneously consider two variables, such the particle size and fracture energy in the PBE, which is addressed in this article. A further challenge would be to combine the PBE with a simulation tool to predict the solid property by considering the impact energy spectra.

Crespo[10] solved a discretized form of the homogeneous bivariate PBE. However, this method only considers a few size and fracture energy intervals and cannot easily be coupled to CFD code if flow or impact energy heterogeneities must be considered.

In this work, the batch grinding equation is solved by the direct quadrature method of moments (DQMOM); one of the advantages of this method is that it can solve the PBE by incorporating several properties of the solid phase. In the QMOM or DQMOM approaches, the mixed moments of the density distribution must be expressed by the quadrature formula by incorporating the weights and abscissas defined for each property. Over the last decade, QMOM and DQMOM modeling methods have been successfully used for a variety of particulate processes: aggregation and breakage processes in homogeneous or one-dimensional flows,[18–20] growth and crystallization processes,[21] coagulation and sintering,[22] and nanoparticle processes,[23] among others. Examples of the use of these methods have also been reported for other dispersed systems, such as liquid sprays undergoing droplet coalescence and evaporation,[24] bubble coalescence and breakage in vertical gas-liquid flows,[25,26] or in stirred tank reactors.[27–29] The breakage phenomena in dispersed systems have thus been intensively treated in the literature by QMOM and DQMOM models. However, the breakage kernels used in these previous studies were usually different from those commonly used in comminution processes and did not consider two properties for the solid phase, such as the particle size and strength; the second being a complex property conditioned by the first. Moreover, another advantage of the DQMOM method is that it solves the spatial and temporal transport equations directly on weights and abscissas, which allows the implementation of the population balance model in CFD codes.[30–33] Thus, DQMOM model provides a promising approach for prospective studies on heterogeneous comminution processes.

In this study, the DQMOM method was used to solve the PBE applied to homogeneous batch grinding processes. In the first step, a single variable, the particle size, is considered, and the results of the model were compared to an analytical solution of the mass balance equation. In the second step, a bivariate model is developed to track the change in the density distribution, which was simultaneously expressed in terms of the particle size and strength. The results of the model are compared with a discretized solution of the PBE by taking a finite number of size and energy intervals. Finally, the benefit of the bivariate approach is discussed based on the sensitivity of the results to the kinetic parameters of the grinding process.

Monovariate DQMOM Applied to Comminution Processes

General equations: homogeneous breakage

For sake of simplicity, only the homogeneous equation of population balance is addressed. The population balance can be expressed as follows by introducing the particle size x and the mass particle-size distribution $f(x, t)$ instead of the number-density function

$$\frac{\partial f(x,t)}{\partial t} = S_x(x,t) \tag{1}$$

In the case of pure breakage, the right-hand side contains only two components, a sink term expressing the breakage of particles of size x in smaller ones and a source term due to the breakage of particles larger than x

$$\frac{\partial f(x,t)}{\partial t} = -a(x)f(x,t) + \int_x^\infty a(y)b(x,y)f(y,t)dy \tag{2}$$

The DQMOM method is based on the Gaussian quadrature.[20,22] The continuous size distribution can then be substituted with the discrete decomposition

$$f(x,t) = \sum_{\alpha=1}^{N} w_\alpha(t)\delta[x(t) - x_\alpha(t)] \tag{3}$$

where N is the number of nodes α, x_α is the property of the node (its size), w_α is its weight, and δ is the Dirac function. If this discrete expression of the mass particle-size distribution $f(x, t)$ is injected into transport Eq. 2, one obtains the following

$$\sum_{\alpha=1}^{N} \delta(x - x_\alpha)\frac{\partial w_\alpha}{\partial t} - \sum_{\alpha=1}^{N} \delta'(x - x_\alpha)w_\alpha \frac{\partial x_\alpha}{\partial t} = S_x(x,t) \tag{4}$$

Following Marchisio and Fox,[20] one can substitute the weighted abscissa, c_α, for the abscissa, x_α, which yields the following

$$c_\alpha = w_\alpha x_\alpha \tag{5}$$

Equation 4 then takes the following form

$$\sum_{\alpha=1}^{N}[\delta(x-x_\alpha)+\delta'(x-x_\alpha)x_\alpha]\frac{\partial w_\alpha}{\partial t}-\sum_{\alpha=1}^{N}\delta'(x-x_\alpha)\frac{\partial c_\alpha}{\partial t}=S_x(x,t) \tag{6}$$

The derivatives with time of both the weights and the weighted abscissa are independent of x. Thus, a set of ordinary differential equations is usually defined to follow the transient changes of these weights and weighted abscissas

$$\frac{\partial w_\alpha}{\partial t}=E_{w\alpha}(t) \qquad \frac{\partial c_\alpha}{\partial t}=E_{c\alpha}(t) \tag{7}$$

The integer moments of the distribution were defined by Hulburt and Katz[34] as follows

$$m_k(t)=\int_{-\infty}^{+\infty}x^k f(x,t)dx=\sum_{\alpha=1}^{N}w_\alpha x_\alpha^k \tag{8}$$

Equation 6 can be transformed into a transport equation of moments by multiplying it by x^k and integrating over x. Different terms need thus to be derived, such as

$$\int_{-\infty}^{+\infty}x^k\delta(x-x_\alpha)dx=x_\alpha^k \tag{9}$$

$$\int_{-\infty}^{+\infty}x^k\delta'(x-x_\alpha)dx=-kx_\alpha^{k-1} \tag{10}$$

Thus, the final equation can be written as follows

$$(1-k)\sum_{\alpha=1}^{N}x_\alpha^k\,E_{w\alpha}+k\sum_{\alpha=1}^{N}x_\alpha^{k-1}\,E_{c\alpha}=\int_{-\infty}^{+\infty}x^k\,S_x(x,t)dx \tag{11}$$

This set of Eq. 11 corresponds to an algebraic system, with $2N$ unknowns: E_{w1}, …, E_{wN}, E_{c1}, …, E_{cN}. Following Marchisio and Fox,[20] one can write this system in matrix form $A\,E=D$, where A is a square matrix *(2N, 2N)* and E and D are column vectors of size $2N$. Thus, $2N$ moments are needed to close the system, so k must vary between 0 and $2N-1$. One can consider two particular values of k, namely $k=0$ and $k=1$.

When $k=0$, the previous equation simplifies to the following form

$$\sum_{\alpha=1}^{N}E_{w\alpha}=\int_{-\infty}^{+\infty}S_x(x,t)dx=0 \tag{12}$$

On the right hand side, the summation of the source and sink terms over the whole distribution of sizes must be null, irrespective of the kernel. Keeping in mind the definition of $E_{w\alpha}$, one can rewrite this expression as follows

$$\frac{\partial}{\partial t}(w_1+w_2+w_3)=\frac{\partial m_0}{\partial t}=0 \tag{13}$$

This result is obvious.

When $k=1$, the previous equation reduces to

$$\sum_{\alpha=1}^{N}E_{c\alpha}=\int_{-\infty}^{+\infty}x\,S_x(x,t)dx=\overline{S_1} \tag{14}$$

Here, one can rewrite this expression as follows by again keeping in mind the definition of $E_{c\alpha}$

$$\frac{\partial}{\partial t}(w_1x_1+w_2x_2+w_3x_3)=\frac{\partial m_1}{\partial t}=\overline{S_1} \tag{15}$$

The transient change in the first moment could be predicted depending on the closure of the sink and source terms. The kernels associated with the present comminution process will be defined in the next paragraph.

Monovariate DQMOM validation and discussion

In the specific case where the selection function $a(x)$ is a power function (Eq. 16) and the breakage distribution function $B(x, y)$ is self-similar as in Eq. 17[7,35–37]

$$a(x)=A_0\left(\frac{x}{x_{\max}}\right)^{a_0} \tag{16}$$

$$B(x,y)=\left(\frac{x}{y}\right)^{a_0} \quad \text{or} \quad b(x,y)=\frac{dB(x,y)}{dx}=\frac{a_0}{y}\left(\frac{x}{y}\right)^{a_0-1} \tag{17}$$

Then, the batch grinding equation has been shown to have an analytical solution

$$R(x,t)=R(x,0)\exp\left(-A_0\left(\frac{x}{x_{\max}}\right)^{a_0}t\right) \tag{18}$$

where $R(x, t)$ is the retained cumulative-size distribution defined as follows

$$R(x,t)=\int_x^{\infty}f(y,t)dy \tag{19}$$

The DQMOM model was developed using Matlab and validated considering a normal law for the initial particle-size distribution with a mean value (m) equal to 3 and a standard deviation (σ) of 0.5. If the order N of the quadrature is chosen to be 3, the weights and abscissas can be calculated as function of the mean and standard deviation of the normal law by the following formula

$$\begin{aligned} x_1(0)&=m-\sqrt{3}\sigma=2.13 & w_1(0)&=1/6\\ x_2(0)&=m=3 & w_2(0)&=2/3\\ x_3(0)&=m+\sqrt{3}\sigma=3.87 & w_3(0)&=1/6 \end{aligned} \tag{20}$$

It corresponds to the following expression for the mass particle-size initial distribution $f(x, 0)$

$$f(x,0)=\frac{1}{\sigma\sqrt{2\pi}}e^{-\frac{(x-m)^2}{2\sigma^2}} \tag{21}$$

One can thus explicitly define the analytical expression of the initial cumulative size distribution $R(x, 0)$ as follows

$$R(x,0)=\int_x^{\infty}f(y,0)dy=\frac{1}{2}\left[1-erf\left(\frac{x-m}{\sqrt{2}\sigma}\right)\right] \tag{22}$$

The analytical solution of the mass particle-size distribution $f(x, t)$ can be expressed as follows

$$\begin{aligned} f(x,t)=&\frac{1}{\sigma\sqrt{2\pi}}e^{-\frac{(x-m)^2}{2\sigma^2}}e^{-A_0\,t\left(\frac{x}{x_{\max}}\right)^{a_0}}+A_0\,t\,a_0\frac{x^{a_0-1}}{{x_{\max}}^{a_0}}\\ &\frac{1}{2}\left[1-erf\left(\frac{x-m}{\sqrt{2}\sigma}\right)\right]e^{-A_0t\left(\frac{x}{x_{\max}}\right)^{a_0}} \end{aligned} \tag{23}$$

The model was validated by comparing the values of the first moments obtained by the DQMOM model with those derived from the analytical solution (Eq. 23). The results reported in Figures 1–3 correspond to the case where A_0 = 0.5 min^{-1} and $a_0=2$. Figure 1a represents the change in the first six moments as a function of time. Due to the definition

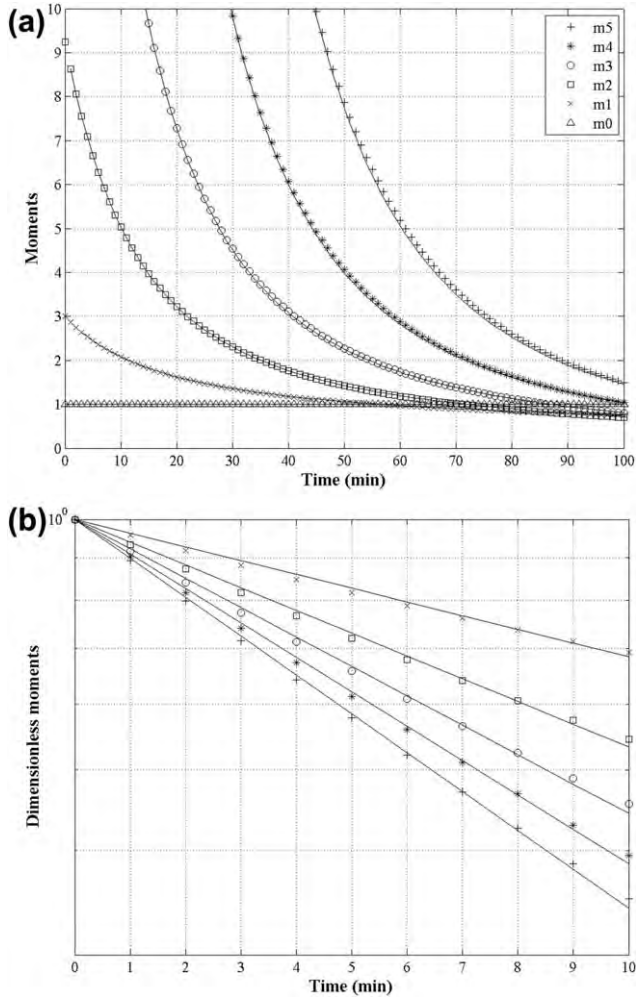

Figure 1. (a) Change in the first moments vs. time—comparison of the monovariate DQMOM solution (points) with the analytical solution (continuous lines) and (b) change in the dimensionless moments at the beginning of the process—comparison of the monovariate DQMOM solution (points) with an exponential law (lines).

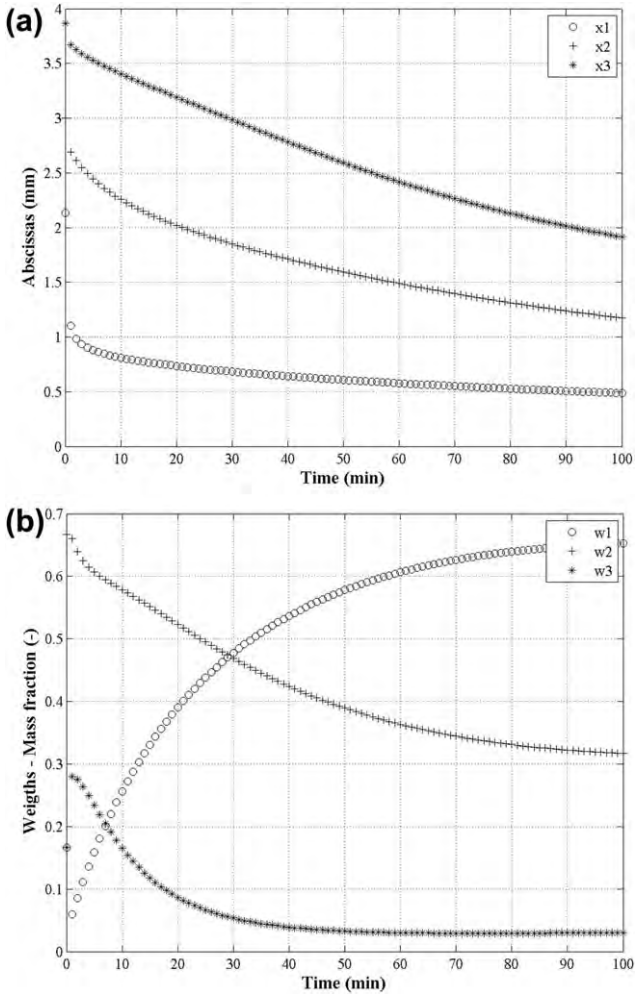

Figure 2. (a) Change in the abscissas—monovariate DQMOM and (b) change in the weights—monovariate DQMOM.

of $f(x, t)$, m_0 represents the overall solid mass and remains constant over time (see Eq. 13), which agrees with the mass conservation during the grinding process. The higher order moments decrease over time due to the size reduction. The simulated values closely approximated the analytical solution. The changes in the dimensionless moments, which were obtained by dividing the transient moments by their value at the initial time, are reported in Figure 1b on a semi-log graph for the first minutes of the process.

In theory, one can return to the conclusions reached in the previous section given the selection and breakage kernels and explicitly define the transient changes in the moments

$$\frac{\partial m_1}{\partial t} = \overline{S_1} = -\frac{A_0}{a_0+1}\frac{1}{{x_{\max}}^{a_0}} m_{a_0+1} \tag{24}$$

The following can be shown in a more general way

$$\frac{\partial m_i}{\partial t} = \overline{S_i} = -i\frac{A_0}{a_0+i}\frac{1}{{x_{\max}}^{a_0}} m_{a_0+i} \tag{25}$$

An analytical expression of the moments as a function of time is not easily derived from these equations. However, an approximated expression of the first moments can be written over the first minutes of the process, as shown in Figure 1b

$$\frac{m_k(t)}{m_k(0)} = \exp\left(-\frac{t}{\tau_k}\right) \tag{26}$$

The time-scale of the local disintegration phenomena given by $1/A_0$ can be compared with the time-scale of the process estimated from τ_k (for $t = \tau_k$, the dimensionless moments are equal to 36.8%). The estimated values obtained for different values of A_0 are reported in Table 1. The time-scale of the process always significantly exceeded the time-scale of the disintegration process, irrespective of the value of A_0. Furthermore, quasi-identical values of the parameters τ_k can determined as a function of the time-scale of the local disintegration phenomena. Specifically, the following relationships could be determined

$$\tau_1 \approx \frac{11.2}{A_0}; \quad \tau_2 \approx \frac{7.2}{A_0}; \quad \tau_3 \approx \frac{5.9}{A_0}; \quad \tau_4 \approx \frac{5.0}{A_0}; \quad \tau_5 \approx \frac{4.4}{A_0} \tag{27}$$

Monovariate DQMOM results and discussion

The changes in the abscissas and weights as a function time are, respectively, reported in Figures 2a, b. As expected,

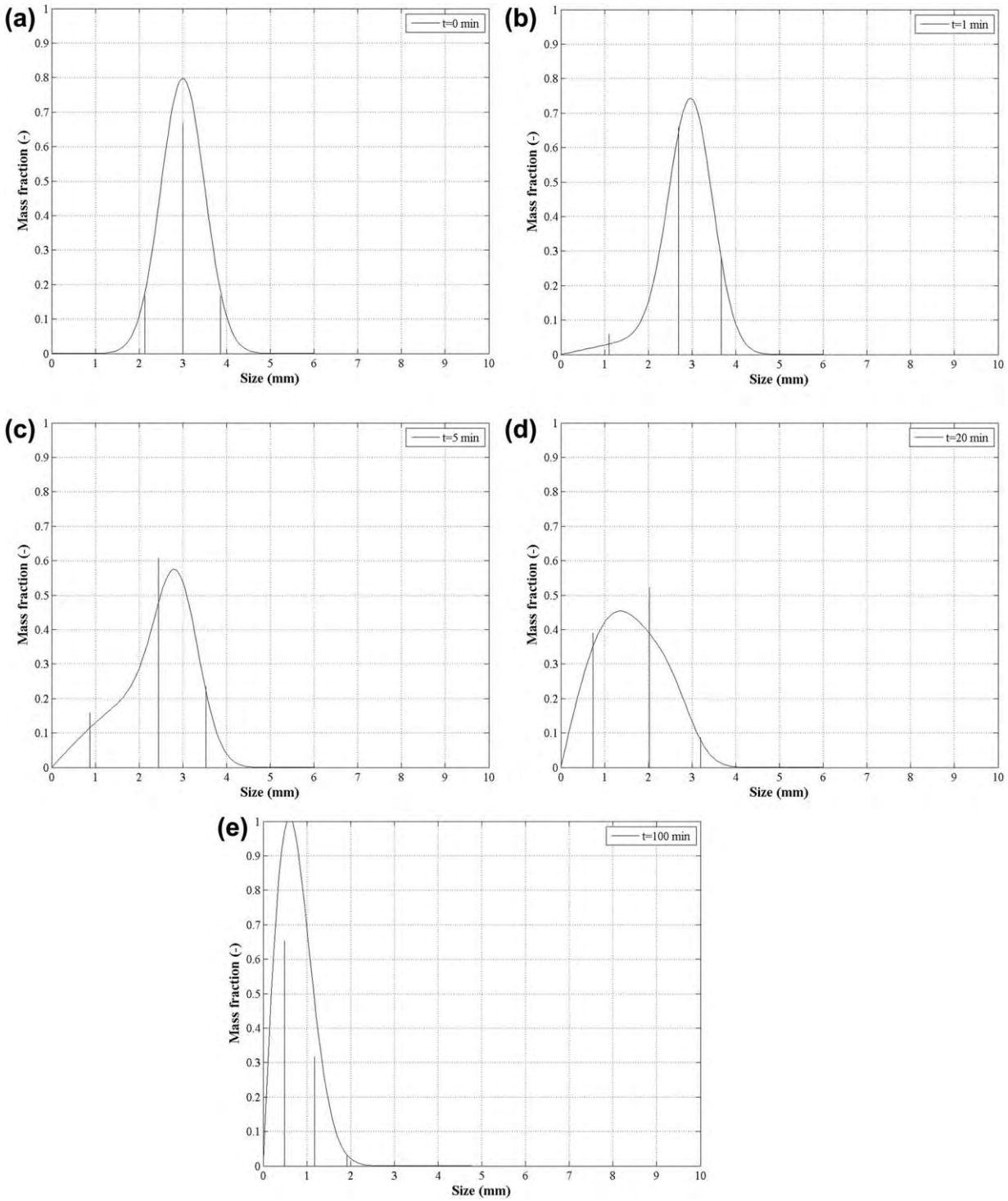

Figure 3. (a) Change in the PSD vs. time (analytical solution) and visualization of couples (w_α, x_α) obtained by DQMOM monovariate—$t = 0$ min, (b) $t = 1$ min, (c) $t = 5$ min, (d) $t = 20$ min, and (e) $t = 100$ min.

Table 1. Comparison of the Time-Scale of the Local Break-Up Phenomena with the Time-Scale of the Grinding Process

Kinetic Parameter A_0 (min^{-1})	Time-Scale Local Break-Up (min)	Time-Scale of the Process (min)				
		τ_1	τ_2	τ_3	τ_4	τ_5
1	1	13.5	8.2	6.3	5.4	4.8
0.5	2	26.3	15.9	12.3	10.5	9.3
0.1	10	111.1	71.4	58.8	50.0	43.5

the abscissas decrease over time in relation to the size reduction process. Simply, if we assume that each couple (x_i, w_i) characterizes a subpopulation of the entire size distribution, their change over time can be compared with the corresponding analytical particle-size distribution. Some examples are given in Figure 3. At each time considered, the abscissas belong to the size range, and the weights agree with the proportion of particles in the entire size distribution. Moreover, Figure 2b shows that the weight of the finer population first decreases during the first minutes of the process before increasing for longer times. Initially, the PSD is narrow, but it rapidly spreads over time as finer fragments are produced. These fragments eventually comprise the finer subpopulation, and the couple (x_1, w_1) reproduces their change. Meanwhile, the weight of the coarser population first increases from its initial value before decreasing. This phenomenon results from the spreading of the PSD; the couple (x_3, w_3) that represents the coarser population at any time expresses this trend. Initially, w_3 equals 1/6, it increases during the first minutes of the process while x_3 decreases (see e.g., Figure 3b at $t = 1$ min) and then decreases as the coarse particles disintegrate. Thus, even though the weights and abscissas do not fully describe the particle-size distributions, these values closely approximate the corresponding analytical PSD.

Bivariate DQMOM Applied to Comminution Process

General equations: homogeneous breakage

Two properties were considered for the solid phase of the bivariate case, the particle size and the particle strength, which was represented by the fracture energy, that is, the minimum energy needed to break the particle. The particle-size energy distribution $f(x, e, t)$, which represents the mass fraction of particles characterized by size x and fracture energy e at instant t, was again approximated based on the N nodes of the Gaussian quadrature

$$f(x,e,t)=\sum_{\alpha=1}^{N} w_\alpha(t)\delta(x-x_\alpha)\delta(e-e_\alpha) \tag{28}$$

Furthermore, the mixed moments were defined as follows

$$m_{kl}(t)=\int_{-\infty}^{+\infty} x^k e^l f(x,e,t)dx=\sum_{\alpha=1}^{N} w_\alpha x_\alpha^k e_\alpha^l \tag{29}$$

In this bivariate case, the ODE system is based on $3N$ equations corresponding to the N nodal values of the weights, weighted sizes, and weighted energies

$$\frac{\partial w_\alpha}{\partial t}=E_{w\alpha} \tag{30}$$

$$\frac{\partial(w_\alpha x_\alpha)}{\partial t}=E_{wx\alpha} \tag{31}$$

$$\frac{\partial(w_\alpha e_\alpha)}{\partial t}=E_{we\alpha} \tag{32}$$

The right hand sides of this ODE system are solutions of the algebraic system with $3N$ unknowns: $E_{w1}, \ldots, E_{wN}, E_{wx1}, \ldots, E_{wxN}, E_{we1}, \ldots, E_{weN}$. The generic equation to build the system is written as follows

$$\sum_{\alpha=1}^{N}\left[(1-k-l)x_\alpha^k e_\alpha^l E_{w\alpha}+kx_\alpha^{k-1}e_\alpha^l E_{wx\alpha}+lx_\alpha^k e_\alpha^{l-1}E_{we\alpha}\right] = -\sum_{\alpha=1}^{N} w_\alpha x_\alpha^k e_\alpha^l a_\alpha+\sum_{\alpha=1}^{N} a_\alpha \overline{b_\alpha}^{kl} w_\alpha \tag{33}$$

The building of this algebraic system corresponds to the choice of $3N$ mixed moments or $3N$ couples (k, l), which are needed to close the system.

Application of bivariate DQMOM: case study

Recall the general mass balance equation for a batch grinding process

$$\frac{\partial f(x,e,t)}{\partial t}=-a(x,e)f(x,e,t) + \int_0^{+\infty}\int_x^{x_{\max}} S(x_0,e_0)b(x,e,x_0,e_0)f(x_0,e_0,t)dx_0\,de_0 \tag{34}$$

Crespo[10] recently developed both experimental and theoretical background for the comminution mechanisms related to this problem. In our bivariate approach, the selection function and the breakage function being based on both size and energy enable to introduce improved physics compared to monovariate case. The selection function $a(x, e)$ describes the rate at which particles of size x and breakage energy e are broken. The breakage function $b(x, e, x_0, e_0)$ represents the probability to obtain fragments of properties (x, e) after a fracture event of particles characterized by size x_0 and breakage property e_0.

Following Crespo,[10] the selection function can be considered as the product of two probabilities: the impact probability, which depends on the process conditions and the particle size, and the breakage probability after a stress event, which depends on the breakage energy. Assuming that the impact probability can be expressed by a power law function as in the previously considered monovariate case (Eq. 16), and that the breakage probability can be described by an exponential law, the overall selection function can be written as follows

$$a(x,e)=A_0\left(\frac{x}{x_{\max}}\right)^{a_0}\left[\exp\left(-\frac{e}{e*}\right)\right] \tag{35}$$

e^* is a reference parameter that as the same dimensions as energy. Its value will be commented on in section Comparison of Monovariate and Bivariate DQMOM Methods.

Similarly, the breakage function can be decomposed into two contributions. Assuming that the size and energy of daughter particles do not depend on the mother energy after breakage, the following equation can be addressed

$$b(x,e,x_0,e_0)=b_1(x,x_0)b_2(e|x) \tag{36}$$

The first term breaks the usual probability into fragments of size x from mother particles of size x_0, as expressed by Eq. 17. The second term expresses the energy spectrum of daughter particles conditioned by their size. The particle fracture energy can be evaluated from single-particle impact test, such as with the UFCL.[11,12] Such experiments conducted on individual particles lead to a large scatter of the data and are usually treated using statistical tools. The

fracture probability can then be described by a log-normal distribution

$$P(E|x)=\frac{1}{2}\left[1+erf\left(\frac{\ln(E/E_{50})}{\sqrt{2\sigma_E{}^2}}\right)\right] \tag{37}$$

where E is the mass-specific particle fracture energy (equal to the particle fracture energy divided by the mass of a particle, e/m_{p}). E_{50} and σ_E are the median and geometric variance of the distribution, respectively. Tavares and King[12] analyzed the effect of the particle size on the fracture energy for a variety of materials, and the following equation for the nominal size was proposed

$$E_{50}=e_{50}/m_p=E_\infty\left[1+\left(\frac{x'}{x-x''}\right)^\phi\right] \tag{38}$$

All parameters in this equation are constants that depend on the material properties. In our simulations, the following data obtained by Tavares and King[12] for irregular particles of quartz were used: $E_\infty = 43.4$ mJ/g, $x' = 3.48$ mm, $x'' = 5$ μm, and $\phi = 1.61$.

The fracture energy spectrum is then given by the following

$$b_2(e|x,t)=\frac{\partial P(e|x)}{\partial e}=\frac{\exp\left[-\frac{(\ln(e/e_{50}))^2}{2\sigma_E{}^2}\right]}{e\sqrt{2\pi\sigma_E{}^2}} \tag{39}$$

With these assumptions, the fracture energy is a function of the particle size and the energy spectrum of the daughter particles does not depend on the mother energy spectrum. The second property of the solid is thus conditioned by the first one and the bivariate PBE could be solved with a conditional quadrature method of moments whose an algorithm was developed by Yuan and Fox.[38] But the choice of DQMOM method rather than CQMOM method is driven by the prospect to derive a general approach of comminution problems that should be transferable to other kind of breakup mechanisms. Indeed, the conditions chosen for the case study are not universal in the comminution context and both properties have been treated here as if they were independent. Thus, the bivariate model could be used in more general situations, when the energy spectrum is not (or not only) governed by the particle size (fatigue phenomena, increase of particle strength, change in fracture mechanism during the process ...) or even when another solid property, such as a morphological parameter, has to be considered.

Bivariate DQMOM validation and discussion

The PBE applied to a bidimensional comminution process does not have an analytical solution, such as the previously defined solution for the monovariate case. To validate the method, the change in certain mixed moments calculated by the bivariate DQMOM were compared to those calculated using a discrete solution of Eq. (34). After the discretization of the variables size and energy, Eq. (34) can be rewritten in the following form

$$\frac{\partial f(i,j,t)}{\partial t}=-f(i,j,t)a(i,j)+\sum_{i_0<i}\sum_{j_0}f(i_0,j_0,t)a(i_0,j_0)b(i,j,i_0,j_0) \tag{40}$$

while considering discrete forms for the selection and the breakage functions such as

$$a(i,j)=A_0\left(\frac{x_i}{x_{\max}}\right)^{a_0}\left[\exp\left(-\frac{e_j}{e*}\right)\right] \tag{41}$$

$$b(i,j,i_0,j_0)=b_1(i,i_0)b_2(j|i)=\frac{a_0}{x_{i0}}\left(\frac{x_i}{x_{i0}}\right)^{a_0-1}b_2(j|i) \tag{42}$$

with

$$e_j=e_{50}(i)\exp\left[\sqrt{2\sigma_E{}^2}\ erfinv\left(2P_j-1\right)\right] \tag{43}$$

$$e_{50}(i)=\beta\rho x_i^3E_\infty\left[1+\left(\frac{x'}{x_i-x''}\right)^\phi\right] \tag{44}$$

$$b_2(j|i)=\frac{1}{\sqrt{2\pi\sigma_E^2}}\frac{1}{e_j}\exp\left[-\frac{\log^2\left(e_j/e_{50}(i)\right)}{2\sigma_E^2}\right] \tag{45}$$

The problem was solved by considering one hundred size intervals between the minimum and maximum sizes (i.e., zero and 6 mm in the studied case) and one hundred energy intervals. The reference energy was defined to be equal to the median energy for the maximum particle size E_{50} ($x_{\max} = 6$ mm). The energy range was chosen to obtain a breakage probability between zero and 1 for each size class. The system of ordinary differential equations obtained after discretization was directly solved using the ode45 function of Matlab.

The discrete solution was used to validate the bivariate solution obtained with DQMOM for a number of nodes $N = 3$. Indeed, following Fox and coworkers,[39,40] it is known that, for two solid properties, the minimum number of nodes to be considered to represent correctly the second-order moments is equal to 3. For $N > 3$, it is necessary to take into account mixed moments having higher orders which have no practical interest for the grinding process. The determination of moments with a high order on the base of experimental data could also lead to significant errors and this would constitute an important limitation for validation purpose.

If the number of nodes is equal to three, nine moments are needed to solve the system. In that case, it is known that there is no optimal moment set.[39,40] However, the following set of moments, that was chosen for the DQMOM resolution: (m_{00}, m_{10}, m_{01}, m_{20}, m_{11}, m_{02}, m_{30}, m_{03}, m_{22}), corresponds to a valid moment set, in accordance with the general rules given by Marchisio and Fox.[40] Indeed, all six moments of global order less than or equal to two were chosen (i.e., m_{00}, m_{10}, m_{01}, m_{20}, m_{11}, m_{02}) and the remaining three moments were of global order three for two of them (m_{30} and m_{03}) and of a global Order 4 for the last one (m_{22}). m_{30} and m_{03} were chosen to precisely predict the pure moments of order three, as suggested by Zucca et al.[23] analysis. Pure moments of order two and three are needed to evaluate the d_{32} (ratio of the pure moment of Order 3 on the pure moment of Order 2), which is a characteristic dimension often considered in particulate processes. Moreover, with the set of moments given above, both properties have been equally treated.

The comparison between certain mixed moments calculated by DQMOM with $N = 3$ and those estimated by the discrete solution is illustrated in Figure 4. The initializing values were obtained by resolving the nonlinear system comprised of the $3N$ mixed moments using a Newton–Raphson iterative method. The following initial values were considered for the weights and abscissas: $w_1 = 0.5$, $w_2 = 0.1$, $w_3 = 0.4$; $x_1 = 2.5$, $x_2 = 3.5$, $x_3 = 3.5$; $e_1 = 2.0$, $e_2 = 10$, and $e_3 = 2.7$.

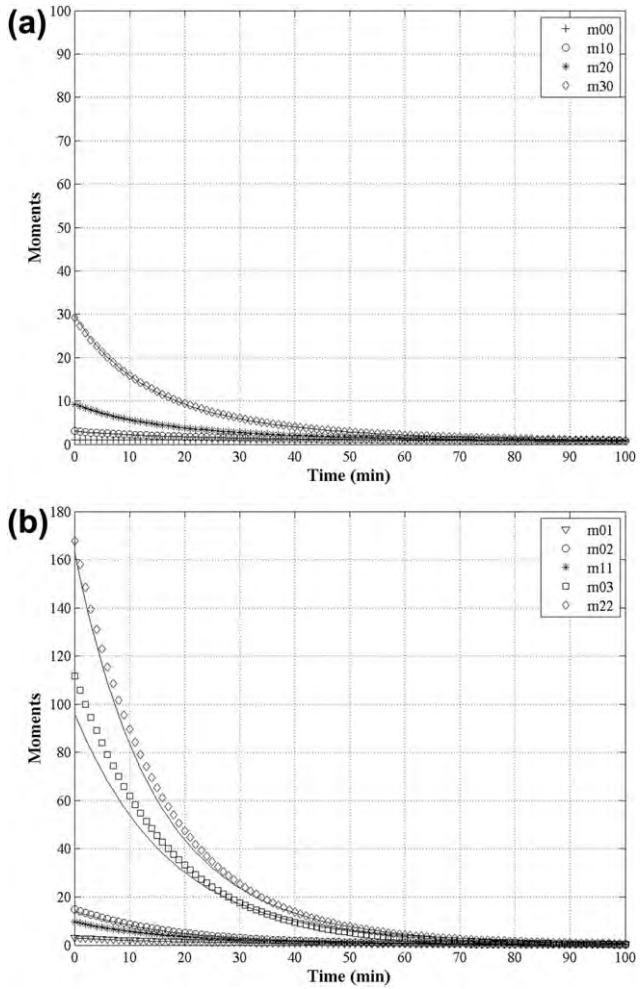

Figure 4. (a) Change in certain mixed moments vs. time–comparison of monovariate DQMOM solution with the discrete solution and (b) change in certain mixed moments vs. time—comparison of bivariate DQMOM solution with the discrete solution.

The models showed significant differences, especially for the mixed moments with a high order on the second variable (see Figure 4b). However, these errors were already present at the initial time. They are due to approximations in the double integral calculation within the discrete solution to determine the mixed moments. The precision of the discrete model could most likely be improved by increasing the number of size and/or energy intervals, which increases the computational time. Indeed, a standard computer obtains the DQMOM solution in a few minutes, whereas the calculation of the discrete model requires approximately two couple of weeks with a 150 × 150 grid. However, similar tendencies can be observed with both models. For example, both models calculated similar values for the Sauter diameter (Figure 5), which is defined by the ratio of the m_{30} to the m_{20} mixed moments.

Moreover, the DQMOM model provides access to the weights and abscissas as a function of time. These data are not directly correlated with the physical properties of the distributions but the couples (w_α, x_α) and the particle-size distributions show good agreement. The PSD were determined as a function of time by using the discrete solution and calculating the mean values of the mass fractions over the energy

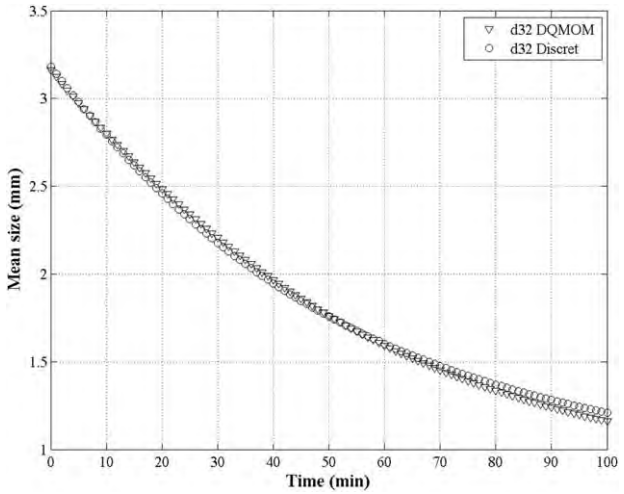

Figure 5. Change in the Sauter diameter vs. time—comparison of bivariate DQMOM solution with the discrete solution.

range. Some examples are reported in Figure 6. The size abscissas belong to the particle-size range, and shifting the abscissas toward the lowest sizes is in concordance with the size reduction process, irrespective of the time. The increase in w_1 also accompanies the creation of a population constituted by fines particles.

Comparison of Monovariate and Bivariate DQMOM Methods

The monovariate and bivariate DQMOM methods can be directly compared by considering the mixed moments with a nil order for the second variable, m_{10}, m_{20}, m_{30}, and so forth for the bivariate solution. The changes in the first six moments over time are reported in Figure 7a. As expected, the moments decrease more slowly with the bivariate solution. The second part of the selection function [$\exp(-e/e^*)$] acts as a decelerator for the breakage process. In the monovariate model, the energy limitation is implicitly contained in the kinetic prefactor A_0. To approach identical conditions, we can assume that the breakage energy is independent of the particle size and constant over time. This constant is termed the critical energy and equal to e^*. If the energy supplied during the process is higher than the critical energy, the breakage probability will equal 1. Conversely, it equals zero when the supplied energy is less than the critical energy. In this case, the energy breakage function can be expressed as follows

$$b(e|x) = \frac{\partial P(e|x)}{\partial e} = \delta(e - e^*) \tag{46}$$

The two models yield very similar values for the transient change of the six moments when the selection function is assumed to only depend on the particle size for both the monovariate and bivariate DQMOM models (Eq. 16) (Figure 7b). Figure 7c also shows that the monovariate and bivariate DQMOM solutions yielded similar changes in the Sauter diameter for the special case of a constant critical energy, whereas these values significantly differ for the general case.

The arbitrary grinding kinetics [$A_0 = 0.5$ min^{-1} and $e^* = e_{50}(x_{\max})$] were considered on the Figure 7c. To prove the benefit of the bidimensionnal model over the

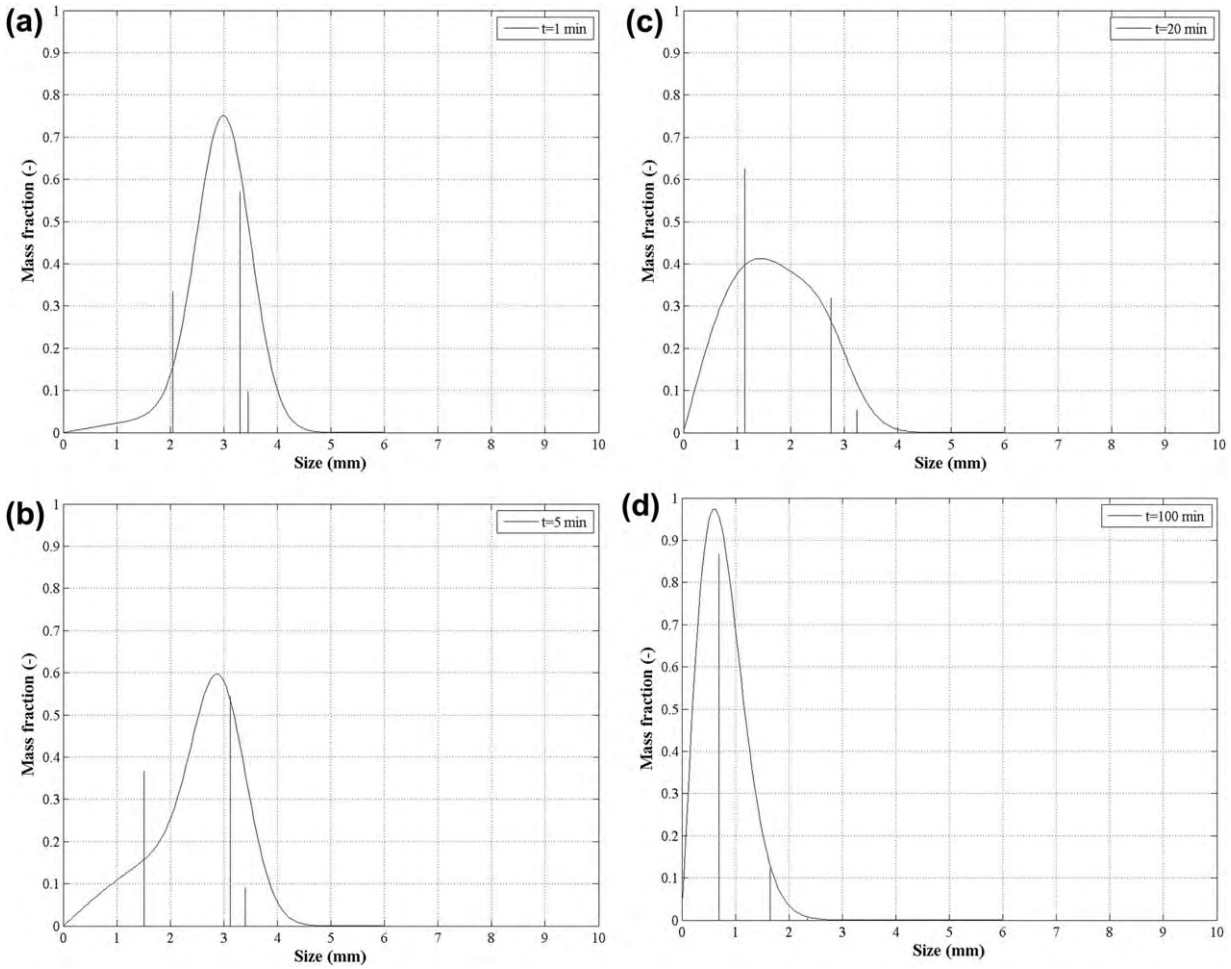

Figure 6. (a) PSD obtained by the discrete solution taking mean values of the mass fractions over the energy range and visualization of the ($w_{\alpha\beta}$ x_α) couples from bivariate DQMOM—$t = 1$ min, (b) $t = 5$ min, (c) $t = 20$ min, and (d) $t = 100$ min.

monovariate model, the transient change in the Sauter diameter calculated with the monovariate model was compared with the solution of the bivariate DQMOM model obtained for different values of the kinetic parameter A_0 while maintaining the reference energy constant (Figure 8a). Similarly, both models were compared for different values of the reference energy Eref while maintaining the kinetic parameter $A_0 = 0.5$ constant (Figure 8b). Decreasing the grinding parameter A_0 decreased the breakage kinetics and dampens the decrease of the Sauter diameter. The difference between the monovariate and bivariate solution was similar irrespective of the value of A_0. In each case, the decrease in the Sauter diameter slowed when considering the energy barrier compared to the solution obtained with the monovariate model.

A similar change was observed when considering the effect of the critical energy, e^*, by dividing or multiplying it by 10. The value of the critical energy significantly affected the Sauter diameter. A low value of the critical energy implies that the material has a low strength (a high grindability) and can be ground by any amount of energy supplied to the mill. If the critical energy is independent of the particle size, the particle strength is not essential to the population balance. On the contrary, the benefit of the bivariate model compared to the classical one becomes significant for hard materials or if the energy needed for breakage depends on the particle size.

Conclusions

The DQMOM was used to solve the PBE applied to a homogeneous batch-grinding process. A property of the solid phase, the particle size, was first considered, and the model was validated by comparing the numerical results with an analytical solution of the PBE obtained by choosing a power law for the size selection function and a self-similarity expression for the breakage function. A bivariate model was then developed in which two properties were considered for the solid phase: the particle size and the minimum energy needed for their breakage. Expressions similar to those of the monovariate case were considered for the selection and breakage-size distribution in this case. Moreover, the energy spectra were assumed to be described by a log-normal probability function, and the breakage energy probability was assumed to be described by an exponential law. The bivariate DQMOM solution was very similar to a discrete solution of the PBE obtained by taking a finite number of size and energy intervals, but the computational time was significantly reduced. Finally, the benefit of the bivariate comminution model was proven by comparing the monovariate and

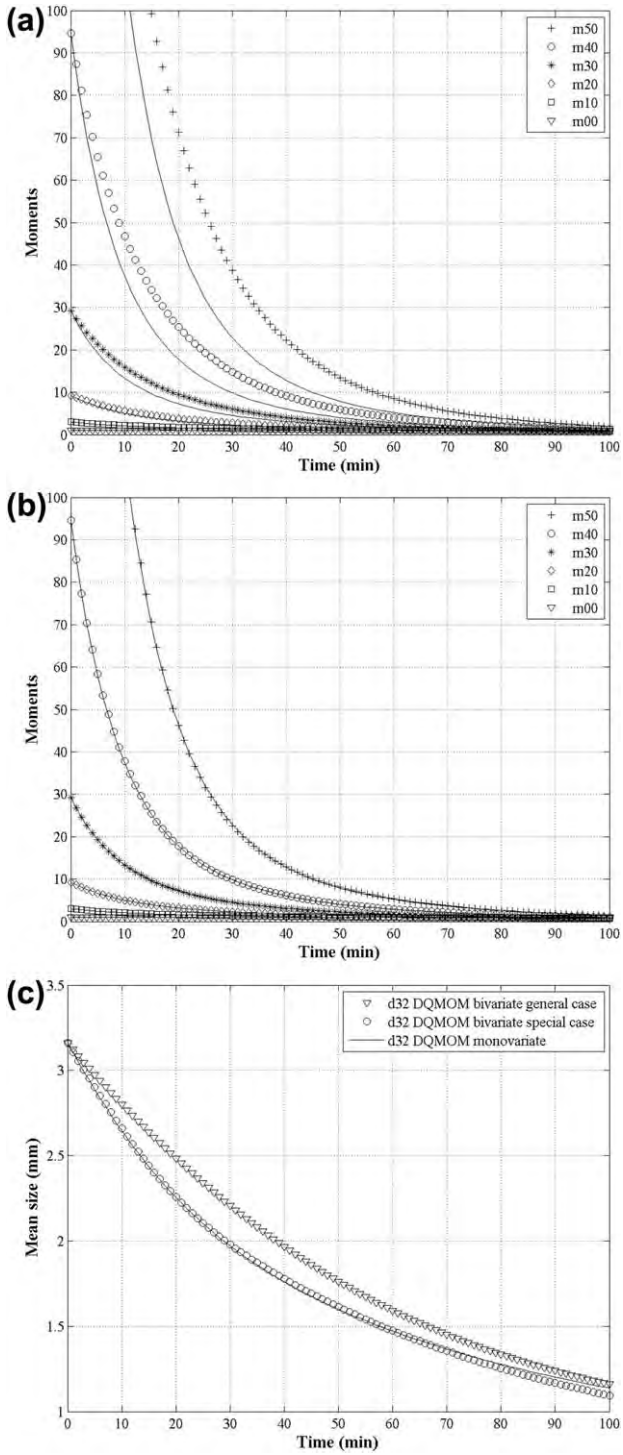

Figure 7. (a) Comparison of monovariate solution and bivariate DQMOM solution in the general case, (b) specific case (Constant critical energy), and (c) comparison of the Sauter diameter obtained with monovariate DQMOM solution and bivariate DQMOM solutions (general and special cases).

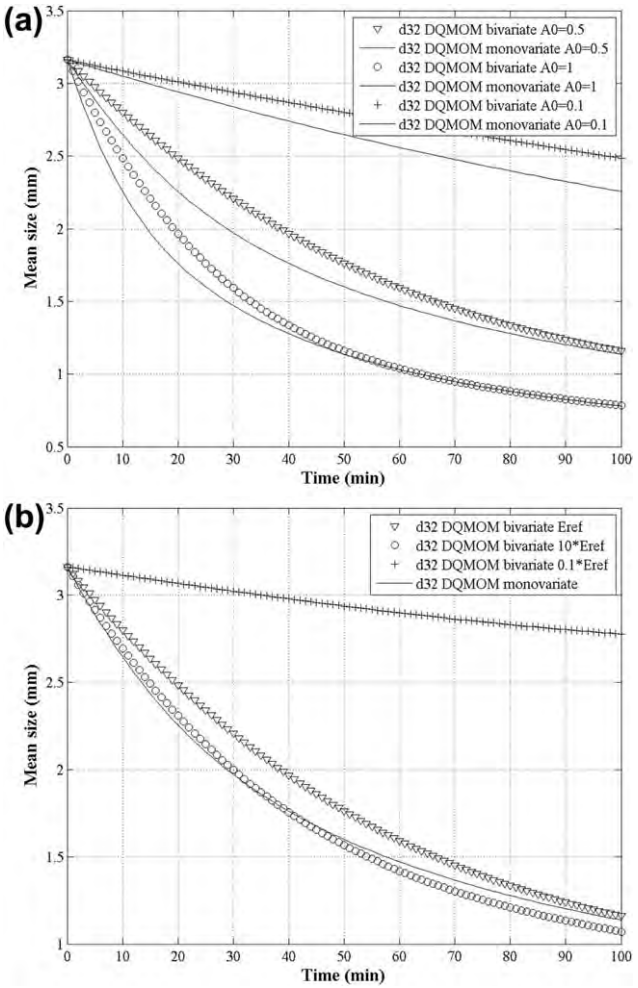

Figure 8. (a) Comparison of the Sauter diameter obtained with monovariate and bivariate DQMOM solutions—effect of A_0 and (b) effect of *Eref*.

bivariate solutions for a simplified case that adopted a critical minimum energy independent of size. The energy needed for breakage can thus be important for hard or heterogeneous materials for which the energy needed for breakage depends on the particle size. Generally speaking, our work shows the applicability of the DQMOM approach to solve a bidimensional PBE for a batch-grinding process. This model could be further developed to implement it in a CFD code to predict the solid properties while considering the heterogeneities of the impact energy inside the grinding chamber. Moreover, this work was focused on the particle size and energy for breakage, but other properties of the solid phase could also be considered. In particular, morphological characteristics could be considered to predict the change in the particle shape during a grinding process.

Literature Cited

1. Lynch AJ. *Mineral Crushing and Grinding Circuits*. New York: Elsevier Scientific Publishing Company, 1977.
2. Prasher CL. *Crushing and Grinding Process Handbook*. New York: Wiley, 1987.
3. Chimwani N, Glasser D, Hildebrandt D, Metzger MJ, Mulenga FK. Determination of the milling parameters of a platinum group minerals ore to optimize product size distribution for flotation purposes. *Miner Eng*. 2013;43/44:67–78.
4. Hennart SLA, Wildeboer WJ, van Hee P, Meesters GMH. Identification of the grinding mechanisms and their origin in a stirred ball mill using population balances. *Chem Eng Sci*. 2009;69(19):4123–4130.
5. Fadda S, Cincotti A, Concas A, Pisu M, Cao G. Modelling breakage and reagglomeration during fine dry grinding in ball milling devices. *Powder Technol*. 2009;194(3):207–216.

6. Hennart SLA, van Hee P, Drouet V, Domingues MC, Wildeboer WJ, Meesters GMH. Characterization and modeling of a sub-micron milling process limited by agglomeration phenomena. *Chem Eng Sci*. 2012;71:484–495.
7. Frances C. On modeling of submicronic wet milling processes in bead mills. *Powder Technol*. 2004;143:253–263.
8. Reid KJ. A solution to the batch grinding equation. *Chem Eng Sci*. 1965;20:953–963.
9. Austin LG, Klimpel RR, Luckie PT. *Process Engineering of Size Reduction: Ball Milling*. New York: Society of Mining Engineers of AIME, 1984:1–561.
10. Crespo EF. Application of particle fracture energy distributions to ball milling kinetics. *Powder Technol*. 2011;210:281–287.
11. King RP, Bourgeois F. Measurement of fracture energy during single-impact fracture. *Miner Eng*. 1993;6:353–367.
12. Tavares LM, King RP. Single-particle fracture under impact loading. *Int J Miner Process*. 1998;54:1–28.
13. Kwade A. Determination of the most important grinding mechanism in stirred media mills by calculating stress intensity and stress number. *Powder Technol*. 1999;105:382–388.
14. Tuzcu ET, Rajamani RK. Modeling breakage rates in mills with inpact energy spectra and ultrafast load cell data. *Miner Eng*. 2011; 24(3/4):252–260.
15. Tuzcu ET, Rajamani RK, Mishara B. Modeling ball mills and semi-autogeneous mills with impact energy spectra-based population balance concept. In: Young CA, Luttrell GH, editors. Separation Technologies for Minerals, Coal and Earth Resources. Society for Mining Metallurgy & Exploration, 2012:695–698.
16. Lane GL. CFD modeling of a stirred bead mill for fine grinding. In *Second International Conference on CFD in the Minerals and Process Industries CSIRO*. Melbourne, Australia, 1999, December 6–8.
17. Gers R, Climent E, Legendre D, Anne-Archard D, Frances C. Numerical simulation of grinding in a stirred media mill: hydrodynamics and collision characteristics. *Chem Eng Sci*. 2010;65:2052–2064.
18. Marchisio DL, Vigil RD, Fox RO. Quadrature method of moments for aggregation-breakage processes. *J Colloids Interface Sci*. 2003a; 258:322–334.
19. Marchisio DL, Vigil RD, Fox RO. Implementation of the quadrature method of moments in CFD codes for aggregation-breakage problems. *Chem Eng Sci*. 2003b;58:3337–3351.
20. Marchisio DL, Fox RO. Solution of population balance equations using the direct quadrature method of moments. *J Aerosol Sci*. 2005; 36:43–73.
21. Marchisio DL, Pikturna JT, Fox RO, Vigil RD, Barresi AA. Quadrature method of moments for population-balance equations. *AIChE J*. 2003c;49:1266–1276.
22. Fox RO. Bivariate direct quadrature method for coagulation and sintering of particle populations. *J Aerosol Sci*. 2006;37:1562–1580.
23. Zucca A, Marchisio DL, Vanni M, Barressi AA. Validation of bivariate DQMOM for nanoparticle processes simulation. *AIChE J*. 2007;53:918–931.
24. Fox RO, Laurent F, Massot M. Numerical simulation of spray coalescence in an Eulerian framework: direct quadrature method of moments and multifluid method. *J Comput Phys*. 2008;227(6):3058–3088.
25. Deju L, Cheung SCP, Yeoh GH, Tu J. Study of isothermal vertical bubbly flow using direct quadrature method of moments. *J Comput Mutiphase Flows*. 2012;4(1):23–40.
26. Deju L, Cheung SCP, Yeoh GH, Tu J. Capturing coalescence and break-up processes in vertical gas-liquid flows: assessment of population balance methods. *Appl Math Model*. 2013;37:8557–8577.
27. Petitti M, Nasuti A, Marchisio DL, Vanni M, Baldi G, Mancini N, Podenzani F. Bubble size distribution modeling in stirred gas-liquid reactors with QMOM augmented by a new correction algorithm. *AIChE J*. 2010;56:36–53.
28. Buffo A, Vanni M, Marchisio DL. Multidimensional population balance model for the simulation of turbulent gas-liquid systems in stirred tank reactors. *Chem Eng Sci*. 2012;70:31–44.
29. Buffo A, Vanni M, Marchision DL, Fox RO. Multivariate quadrature-based moments methods for turbulent polydisperse gas-liquid systems. *Int J Mutiphase Flow*. 2013;50:41–57.
30. Marchisio DL, Barresi AA. Investigation of soot formation in turbulent flames with a pseudobivariate population balance model. *Chem Eng Sci*. 2009;64(2):294–303.
31. Di Pasquale N, Marchisio DL, Barresi AA. Model validation for precipitation in solvent-displacement processes. *Chem Eng Sci*. 2012; 84:671–683.
32. Silva LFLR, Damian RB, Lage PLC. Implementation and analysis of numerical solution of the population balance equation in CFD packages. *Comput Chem Eng*. 2008;32(12):2933–2945.
33. Silva LFLR, Lage PLC. Development and implementation of a polydispersed multiphase flow model in OpenFOAM. *Comput Chem Eng*. 2011;35(12):2653–2666.
34. Hulburt HM, Katz S. Some problems in particle technology. *Chem Eng Sci*. 1964;19:555–574.
35. Austin LG, Luckie PT, Klimpel RR. Solutions of the batch grinding equation leading to Rosin-Rammler distributions. *Trans AIME*. 1972; 252:87–94.
36. Austin LG, Shoji K, Bhatia VK, Jindal V, Savage K, Klimpel RR. Some results on the description of size reduction as a rate process in various mills. *Ind Eng Chem Process Des Dev*. 1976;15(1):187–196.
37. Kapur PC. Self-preserving size spectra of comminuted particles. *Chem Eng Sci*. 1972;27:425–431.
38. Yuan C, Fox RO. Conditional quadrature method of moments for kinetic equations. *J Comput Phys*. 2011;230:8216–8246.
39. Fox RO. Optimal moment sets for multivariate direct quadrature method of moments. *Ind Eng Chem Res*. 2009;49:9686–9696.
40. Marchisio DL, Fox RO. *Computational Models for Polydisperse Particulate and Multiphase Systems*. Cambridge University Press, Cambridge, 2013.